Electrical Measurement of Spin-Wave Interactions of Proximate Spin Transfer Nanooscillators

M. R. Pufall, W. H. Rippard, and S. E. Russek
Electromagnetics Division, National Institute of Standards and Technology, Boulder, Colorado 80305, USA

S. Kaka
Seagate Technology, Pittsburgh, Pennsylvania 15222, USA

J. A. Katine
Hitachi Global Storage Technologies, San Jose, California 95120, USA
(Received 6 June 2006; published 23 August 2006)

We have investigated the interaction mechanism between two nanocontact spin transfer oscillators made on the same magnetic spin valve multilayer. The oscillators phase lock when their precession frequencies are made similar, and a giant magnetoresistance signal is detectable at one contact due to precession at the other. Cutting the magnetic mesa between the contacts with a focused-ion beam modifies the contact outputs, eliminates the phase locking, and strongly attenuates the magnetoresistance coupling, which indicates that spin waves rather than magnetic fields are the primary interaction mechanism.

DOI: 10.1103/PhysRevLett.97.087206 PACS numbers: 85.75.−d, 05.45.Xt, 75.75.+a

Torques due to the transfer of angular momentum between a spin-polarized electric current and a local magnetic moment—"spin transfer" torques—provide a new method to drive a variety of magnetization dynamics, from magnetic switching [1] and low frequency noise [2] to high frequency, narrow band magnetic precession [3,4], without the use of a time-varying magnetic field. The spin transfer effect relies on large current densities to exert torques on the magnetic moment sufficient to overcome the intrinsic damping torque and is typically achieved by patterning a multilayered magnetic film into pillar structures with $\approx$100 nm diameters (nanopillars) or by employing nanometer-scale electrical contacts to continuous, unpatterned magnetic films (nanocontacts) [3,5]. Spin transfer in a nanocontact induces narrow band (1–50 MHz) microwave (1–40 GHz) precession in a nonlinear amplitude regime. This results in an oscillator that responds nonlinearly to ac currents [6], ac fields, and spin waves propagating into the nanocontact from the surrounding magnetic medium, as we will show here. This interaction causes frequency pulling and phase locking of the oscillator to an ac signal and provides a potential means for frequency mixing, phase control, and coherent power combining of arrays of nanoscale microwave oscillators.

When two closely spaced nanocontacts are made to the same magnetic film and either independently current-biased [7] or connected in parallel [8], the two contacts interact and phase lock. Phase locking is a general characteristic of nonlinear oscillators, with examples occurring across the biological and physical sciences [9]. In a nanocontact, current is injected into a small region of a continuous multilayer film, inducing large-angle precession of the magnetization in the injection region and (potentially) radiation of spin waves into the surrounding ferromagnetic film [10]. The phase locking of closely spaced contacts has been attributed to mode overlap [8], to ac fields generated by the oscillators' time-varying magnetization [11], and to spin-wave coupling [7]. Understanding the true phase locking mechanism and, more generally, the interaction of these nanometer-scale nonlinear oscillators with the surrounding ferromagnetic medium are major outstanding questions for future applications. Here we show that cutting the magnetic mesa between the two contacts eliminates the phase locking, which indicates that spin waves, rather than magnetic fields, are the primary interaction mechanism for contacts spaced greater than 200 nm. We also show that one contact can be used as a giant magnetoresistance (GMR) detector of spin waves radiating from the other, providing a method for electrically probing spin-wave dynamics at nanometer length scales.

The magnetic structures are sputter-deposited spin valves comprising Ta 5 nm/Cu 50 nm/$Co_{90}Fe_{10}$ 20 nm/Cu 5 nm/$Ni_{80}Fe_{20}$ 5 nm/Cu 2 nm/Au [3]. The films were patterned into 8 μm $\times$ 20 μm mesas, and two $\approx$ 50 nm electrically isolated contacts were made to each mesa [7]. The fabricated structures had contact edge-to-edge spacing varying from 150 nm to 1 μm. The thick CoFe layer, with its larger total moment, is relatively immune to spin transfer effects and acts as a spin-polarizing reference layer. The thinner NiFe "free" layer has a lower total moment, making it more susceptible to spin transfer torques. Its motion relative to the CoFe layer changes the device resistance via the GMR effect, causing a changing voltage under current bias.

The measurement schematic is shown in Fig. 1. Each device is independently current-biased, with positive current defined as that driving the spin transfer instability [12]. The ac voltage from each contact is coupled out the capacitive leg of a bias tee, through a microwave switch, and into a coherent power combiner. This allows measurement of the rms power emitted from each device individually or the coherently combined power from both [13].

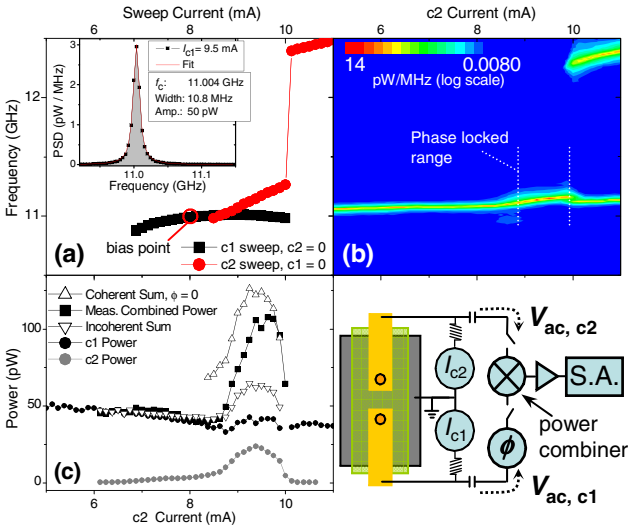

FIG. 1 (color online). Phase locking of two nanocontacts $c1$ and $c2$, spaced at 500 nm. System schematic shown at bottom right. (a) Frequency f vs I for each contact, with other contact at $I = 0$. Inset: Spectrum for $I_{c1} = 9.5$ mA. (b) Contour plot of combined spectral output for $I_{c1} = 8$ mA, I_{c2} swept from 5 to 11 mA. Color denotes measured power. (c) Powers from peak at $\approx$11 GHz in combined, $c1$, and $c2$ outputs during measurement in (b). Circles: Measured powers from each contact. Squares: Measured combined powers. Down triangles: Mathematical sum of $c1$ and $c2$. Up triangles: Coherent sum of $c1$ and $c2$ at zero relative phase.

The combined measured power is $P_{\text{both}} = P_{c1} + P_{c2} + 2(P_{c1}P_{c2})^{1/2}\cos(\phi(t))$, where $\phi(t)$ is the relative phase angle between the devices. If the devices are phase locked, $d\phi/dt = 0$ and the cross term can be nonzero, resulting in an increase (if $|\phi| < \pi/2$) in the measured power over the incoherent sum. A phase shifter permits dc adjustment of the relative phase of the combined signals. All measurements were made at 300 K, with a field of 0.8 T applied 10° from the surface normal, a geometry in which spin waves are radiated from the contact area, according to theory [10,11] and micromagnetic simulations [14].

The spectral output vs current I was measured for each contact, with the other contact held at $I = 0$. By fitting a Lorentzian to the output spectrum measured at a given current [see inset in Fig. 1(a)], the precession frequency, power, and linewidth (FWHM) were determined. The individual output frequencies for two contacts spaced at 500 nm are shown in Fig. 1(a). The observed (and not well understood) output variations are typical of nominally identical nanocontacts [3,6,7], with contact $c1$ (squares) a weak function of current, whereas contact $c2$ (circles) exhibits an abrupt jump at $\approx$ 10 mA. Their frequencies overlap at $\approx$ 11 GHz and should interact and phase lock most strongly there [15]. With contact $c1$ biased to 8 mA (generating output at $\approx$ 11 GHz), the current I_{c2} through contact $c2$ was swept and the spectrum measured as a function of I_{c2} for three configurations: the combined output, the output from $c1$, and the output from $c2$.

The spectrum vs I_{c2} for the coherently combined powers is shown in Fig. 1(b). In the absence of interactions, the combined output would be a superposition of the output from $c2$ [Fig. 1(a)] and a straight line from $c1$, one with positive slope due to the oersted magnetic fields generated by the increasing current through contact $c2$. The plot initially shows a line with small positive slope, but this curve deviates from linearity just below 8.5 mA, accompanied by an increase in power. The frequency pulling and power increase near the crossing point of the individual contact outputs are indicative of phase locking [6,7].

The large power output continues until $I_{c2} \approx 10$ mA, at which there is a split in the spectrum and, subsequently, output at two distinct frequencies. This is due to a jump in the output frequency of $c2$ [see Fig. 1(a)], separating the precession frequencies of $c1$ and $c2$ sufficiently such that they no longer phase lock [6,7,15]. Each then emits a frequency near its individually swept output [Fig. 1(a)]. Measurements of the spectral output from each contact during the same experiment support these suppositions. Contact $c1$ emits the majority of the combined output for $I_{c2} < 8.5$ mA, and both contacts show their largest output from 8.5 to 10 mA (i.e., the locking range). Finally, the signal at 12 GHz for $I_{c2} > 10$ mA is emitted from contact $c2$, while the signal near 11 GHz is emitted by $c1$.

The powers measured from $c1$, $c2$, and the combined outputs in the $\approx$ 11 GHz peak are shown in Fig. 1(c). The power in the intersection region from 8.5 to 10 mA is larger than the incoherent sum of the individual contact outputs, indicating a fixed phase relationship, i.e., phase locking. In this case, the relative phase was $\approx 40° \pm 4°$, determined by fitting (it was not optimized to $2n\pi$ with the phase shifter). Outside the interaction region, the measured combined power is equal to the incoherent sum of the individual powers. Phase locking was not observed for contacts spaced at 1 μm, implying a characteristic locking distance between 0.5 and 1 μm.

To determine the locking mechanism, the magnetic mesa between the two contacts was then cut (see Fig. 2 inset) with a focused-ion beam (FIB). This prevents spin waves from directly coupling the oscillators but would still allow coupling by dipolar magnetic fields generated by the oscillators. The results after FIB cutting of the device measured in Fig. 1 are shown in Fig. 2. In these data, $c2$ is biased to 7 mA, and the current through $c1$ swept. As seen in the spectral outputs in Figs. 2(a)–2(c), with the magnetic mesa cut, the individual contact outputs no longer exhibit frequency pulling as they approach each other, as in the uncut device (see Fig. 1). In addition, the powers no longer combine coherently at the intersection point [see Fig. 2(d)], instead combining to the incoherent sum. These results suggest that the phase locking seen in Fig. 1 is due to spin-wave propagation in the magnetic material.

The output of $c1$ was modified by FIB cutting [compare Figs. 1(a) and 2(b)]. For all but the 1 μm spaced contacts, changes were seen in both contact outputs. Contacts still emitted similar average frequencies but showed differ-

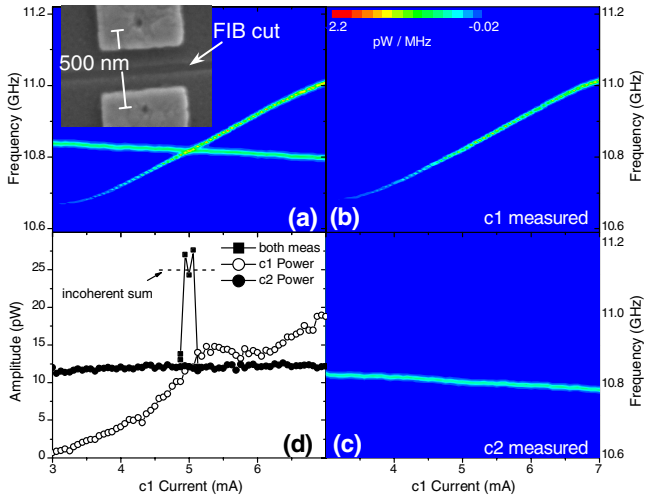

FIG. 2 (color online). Output from device measured in Fig. 1 after FIB cutting. For all panels, current I_{c1} swept, $I_{c2} = 6.75$ mA. (a) Coherently combined powers. Inset: Electron micrograph of contacts showing cut. (b)–(c) Outputs from $c1$ and $c2$, respectively. (d) Measured powers. Circles: Powers from each contact. Squares: Measured combined $c1$ and $c2$ powers. Dotted line: Mathematical (incoherent) sum of $c1$ and $c2$.

ences in their linewidths and frequency vs I dispersions and discontinuities. This is likely due to the creation of a new boundary condition and scattering center less than 250 nm away from the contact, altering the resonance.

FIB cutting also suppressed frequency pulling and phase locking for contacts spaced less than 500 nm apart. For the closest-spaced ($\lesssim$200 nm) contacts, small signals were still detected at one contact due to precession at the other contact after FIB cutting but were over an order of magnitude smaller than similar signals seen in uncut devices [see contact $c2$, $I_{c2} = 6$–8 mA, Fig. 1(c)]. To better quantify the coupling for both uncut and FIB-cut contact pairs, another measurement was performed. First, one contact (hereafter the ''emitter'') was current-biased to induce precession, as before. Then, the current through the second (''detector'') contact was again swept, but in this case the current was swept from negative currents, i.e., currents that *suppress* spin transfer effects by increasing the effective damping [12,16], to positive currents just below the critical current for the onset of precession of that contact. Since spin transfer precession is not induced, the swept contact acts merely as a current-biased GMR detector of either ac fields or spin waves propagating from the emitter contact to the detector contact.

Emitter-detector measurements are shown in Fig. 3 for a 200 nm-spaced uncut contact pair. Figure 3(a) shows the emitter contact output as measured from the emitter itself for an emitter bias current of 6.5 mA, as a function of detector contact current I_d. The emitter frequency increases linearly due to the oersted field from the detector current ramp, while the emitter power is roughly constant. In contrast, the signal at the detector [shown in Fig. 3(b)] is a strong function of I_d: The signal is in the noise at $I_d = 0$ and increases for increasing $|I_d|$, as one would expect for a GMR signal.

Normalizing the detector power to the emitter power [Fig. 3(c), black squares] gives a measure of the detector response for a given emitter amplitude. At this contact spacing, the GMR signal at the detector is less than 5% of the emitter signal. The detector signal drops by an order of magnitude for 500 nm-spaced contacts and is undetectable at 1 μm spacing. Without spin transfer effects, the output power of a GMR sensor is proportional to I_d^2. However, as seen in Fig. 3(c), the detector response is asymmetric with I_d, with positive currents producing larger output. Positive currents produce spin transfer torques that counteract the damping (eventually causing the instability resulting in precession), thus increasing the effective susceptibility of the detector, increasing the response to signals from the emitter. In contrast, negative currents increase the effective damping and lower the susceptibility [12,16].

The second curve in Fig. 3(c) (circles) shows the normalized signal at the detector for 200 nm-spaced contacts after FIB cutting the magnetic mesa. The signal is smaller by over an order of magnitude and is undetectable for negative currents. This result implies that the signal at the detector due to precession at the emitter in the uncut mesa is due primarily to spin-wave propagation through the mesa and demonstrates electrical detection of short wavelength spin-wave radiation with point contact GMR structures. Assuming that the spin-wave wavelength is much larger than the contact, and a GMR $\Delta R_{\max} = 100$ mΩ, we estimate $\approx 2°$ relative motion of the layers at the detector contact for $I_d = 6.5$ mA. Results of this form were seen for all contact pairs. However, variations in the normalized detector signal were observed with field

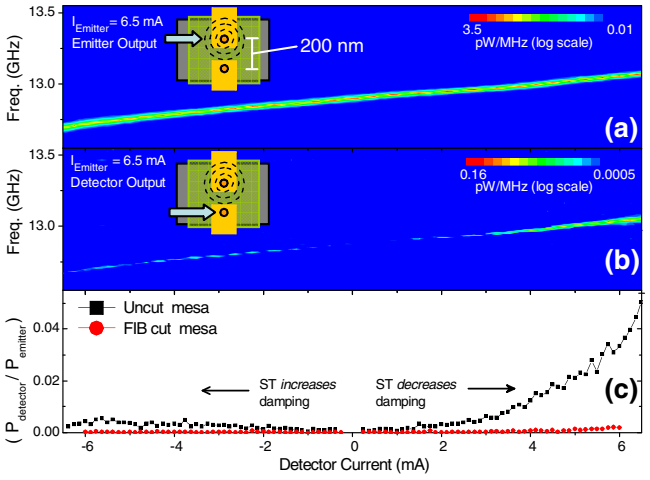

FIG. 3 (color online). Spectrum at one contact (detector) due to precession at the other (emitter), 200 nm separation. Schematics show emitting contact; arrow denotes measured contact. For all plots, $I_{\text{emitter}} = 6.5$ mA. (a) Output from emitter vs I_d. (b) Signal at detector. (c) Normalized power $P_{\text{detector}}/P_{\text{emitter}}$ vs I_d for data in (a) and (b). Also shown: Data for FIB-cut mesa.

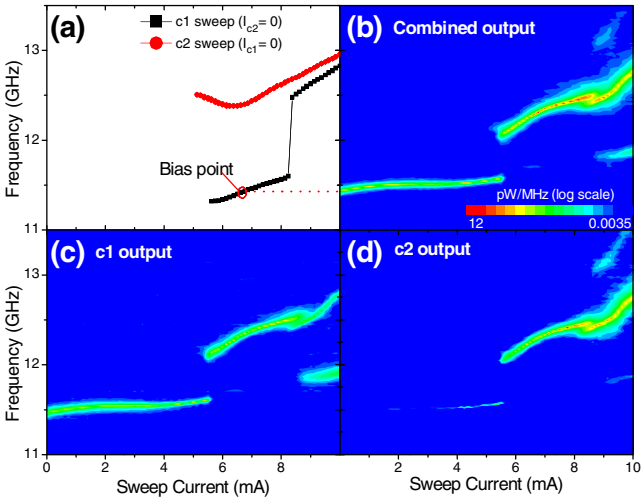

FIG. 4 (color online). Phase locking for 200 nm contact spacing. (a) f vs I for each contact, with the other at $I = 0$. (b) Contour plot of combined spectral output for $I_{c1} = 6.75$ mA, I_{c2} swept. (c),(d) Outputs from contacts $c1$ and $c2$, respectively, for $I_{c1} = 6.75$ mA, $I_{c2} =$ swept.

and geometry for a given spacing, and in the detector signal for a given sample, and are not well understood.

The interactions for closely spaced (<300 nm) uncut devices are strong and cause the contact outputs to deviate considerably from the individual outputs. Furthermore, as shown in Fig. 3, the measured signal from each contact will be a combination of spin transfer precession, GMR due to spin waves from the other contact, and (to a much lesser extent) GMR due to ac magnetic fields. One consequence is that (unlike in Fig. 1) it is more difficult to delineate the locking region. An example for two contacts spaced at 200 nm is shown in Fig. 4. Frequency vs I curves for the individual contacts are shown in Fig. 4(a). I_{c1} is then biased to 6.75 mA and I_{c2} swept. In the combined output [Fig. 4(b)], one initially sees the output solely from $c1$, which then increases nonlinearly in frequency with I_{c2}. At the critical current for precession of $c2$ ($I_{c2} \approx 5.5$ mA), the frequency jumps $\approx$ 500 MHz, accompanied by an increase in power, indicating phase locking. This locked mode increases in frequency until $I_{c2} \approx 8.5$ mA, whereupon it splits into three modes. The magnitude of the jump shows that the interaction is much stronger than for the 500 nm-spaced contacts. This is consistent with the locking seen using nominally identical electrically parallel contacts, which consistently locked only for spacings less than 200 nm [8]. Closely spaced contacts can have large frequency differences and still phase lock.

Figures 4(c) and 4(d) show the respective outputs from $c1$ and $c2$ during this measurement. The combined output for low I_{c2} is primarily from contact $c1$, but, from $I_{c2} >$ 1 mA to the jump at $I_{c2} = 5.5$ mA, a small signal is also measured from $c2$ at the same frequency. This signal may be due to contact $c2$ acting as a GMR sensor of spin waves induced by precession at $c1$, as the current through $c2$ is below the critical current for spin transfer induced oscillations. However, the deviation from linearity of the output frequency vs I_{c2} implies that $c2$ is not acting simply as a detector but is also modifying the precession at $c1$, i.e., quasilocking. This is also seen above the phase locked range for $I_{c2} > 8.5$ mA, but with $c1$ now detecting the spin-wave radiation from the 12.5 GHz mode of $c2$.

In summary, we studied the interaction and phase locking characteristics of two spin transfer oscillators made on the same magnetic multilayer. Cutting the mesa between the contacts greatly attenuated the interactions and eliminated mutual phase locking, which shows that the interaction between contacts at these spacings is primarily via spin waves. One nanocontact was also biased as a GMR sensor and used as an electrical detector of spin waves radiated from a precessional mode excited at the second contact. These measurements provide a means to study spin-wave dynamics on the nanometer length scale and point a way to creating larger systems of phased-array nanooscillators coupled via spin waves.

We thank Tim Cornell and Fred Wiatrowski (Seagate) for the FIB work and T. J. Silva (NIST) for valuable discussions.

[1] J. A. Katine *et al.*, Phys. Rev. Lett. **84**, 3149 (2000); B. Ozyilmaz *et al.*, Phys. Rev. Lett. **91**, 067203 (2003).
[2] M. Tsoi *et al.*, Nature (London) **406**, 46 (2000); S. Urazhdin *et al.*, Phys. Rev. Lett. **91**, 146803 (2003); M. Covington *et al.*, Phys. Rev. B **69**, 184406 (2004).
[3] W. H. Rippard *et al.*, Phys. Rev. Lett. **92**, 027201 (2004).
[4] S. I. Kiselev *et al.*, Nature (London) **425**, 380 (2003).
[5] M. Tsoi *et al.*, Phys. Rev. Lett. **80**, 4281 (1998); T. Y. Chen, Y. Ji, and C. L. Chien, Appl. Phys. Lett. **84**, 380 (2004).
[6] W. H. Rippard *et al.*, Phys. Rev. Lett. **95**, 067203 (2005).
[7] S. Kaka *et al.*, Nature (London) **437**, 389 (2005).
[8] F. B. Mancoff *et al.*, Nature (London) **437**, 393 (2005).
[9] S. Strogatz, *Sync: The Emerging Science of Spontaneous Order* (Hyperion, New York, 2003); R. A. York, IEEE Trans. Microwave Theory Tech. **41**, 1799 (1993).
[10] S. M. Rezende, F. M. de Aguiar, and A. Azevedo, Phys. Rev. B **73**, 094402 (2006); M. A. Hoefer *et al.*, Phys. Rev. Lett. **95**, 267206 (2005); A. N. Slavin and V. S. Tiberkevich, Phys. Rev. Lett. **95**, 237201 (2005).
[11] A. N. Slavin and V. S. Tiberkevich, Phys. Rev. B **72**, 092407 (2005).
[12] J. C. Slonczewski, J. Magn. Magn. Mater. **159**, L1 (1996).
[13] The ac isolation between contacts is over 35 dB.
[14] D. V. Berkov and N. L. Gorn, J. Appl. Phys. **99**, 08Q701 (2006).
[15] P. Hadley, M. R. Beasley, and K. Wiesenfeld, Phys. Rev. B **38**, 8712 (1988).
[16] I. N. Krivorotov *et al.*, Science **307**, 228 (2005).